52nd IEEE Conference on Decision and Control
December 10-13, 2013. Florence, Italy

Comparison between nonlinear model-based controllers and gain-scheduling Internal Model Control based on identified model*

Esmaeil Jahanshahi and Sigurd Skogestad

Abstract— **Instability and inverse response behaviour make anti-slug control at offshore oil-fields an interesting control problem where a robust solution considering the nonlinearity of the system is required. We tested three control solutions by experiments in this paper. First, we used state-feedback with state estimation by a nonlinear high-gain observer. Secondly, we applied feedback linearization with measured outputs. Finally, we designed gain-scheduling IMC (Internal Model Control) based on linear models identified from closed-loop step test. We compared these three solutions in terms of robustness and their range of operation. The high-gain observer was only applicable by using the top-side pressure measurement in a limited range; it was not stable when using the the subsea pressure measurement in closed loop. The IMC method was more robust against time-delay in the subsea pressure measurement compared to the feedback linearizing controller.**

I. INTRODUCTION

Oscillatory slugging flow conditions in offshore multi-phase pipelines are undesirable and an effective solution is needed to suppress them. One way to prevent this behaviour is to reduce the opening of the top-side choke valve. However, this conventional solution increases the back pressure of the valve, and it reduces the production rate from the oil wells. The recommended solution to maintain a non-oscillatory flow regime together with the maximum possible production rate is active control of the topside choke valve [1]. The control system used for this purpose is called anti-slug control. This control system uses measurements such as pressure, flow rate or fluid density as the measured controlled variables and the topside choke valve is the main manipulated variable [2].

Existing anti-slug control systems tend to become unstable after some time, because of inflow disturbances or plant changes. We aim to find a robust control solution for anti-slug control systems. The nonlinearity at different operating conditions is one source of plant change. The effective time delay in the process is another problematic factor for stabilization. In addition, for the topside pressure, there are two unstable (RHP) zeros which result in an inverse response, and make stabilization difficult. The nonlinearity can be counteracted by gain-scheduled linear controllers or by model-based nonlinear controllers. These two approaches are compared in terms of robustness and operation range in this paper, by comparing delay margin of the control loop and the maximum achievable valve opening.

*This work was supported by SIEMENS, Oil & Gas Division

E. Jahanshahi and S. Skogestad are with Department of Chemical Engineering, Norwegian University of Science and technology, Trondheim, NO-7491 skoge@ntnu.no

TABLE I

SUCCESS OF DIFFERENT SOLUTIONS FOR ANTI-SLUG CONTROL

method \ measurement	topside pressure	subsea pressure	using both pressures
PID/$\mathcal{H}_\infty$/LQG [2], [8]	†	☺	☺
Linear observer [6]	†	☺	–
Nonlinear observer [6]	☹	†	†
Feedback linearization [7]	–	–	☺
Back stepping [3]	–	☺	–
IMC [this work]	–	☺	–

–: not investigated ☺: works well ☹: not robust †: doesn't work

A back-stepping design has been used in [3] for nonlinear control of slug flow in risers. A partially linearizing feedback controller that uses the mass of liquid in the riser for state feedback was proposed in [4]. A simple nonlinear Luenberger-type observer was used in [5] to estimate the state variable needed for the controller. However, the *separation principle* does not hold for nonlinear systems in general, and the combined closed-loop observer/controller is not guaranteed to be stable for all conditions. In our previous work [6], it was shown that a nonlinear observer fails in closed-loop when using the subsea pressure as the measurement. This was a surprising result, since the subsea location is preferred when using simple PI control. A nonlinear model-based controller designed using feedback linearization was proposed in [7]. This controller uses the measurements of the system directly, without using any observer. However, the feedback linearization design is not robust against modeling errors, since the nonlinearities of the system must be perfectly known in order to cancel them. A summary of different anti-slug control solutions is given in Table I.

An alternative approach, in which the mechanistic model is not directly used for the control design, is to identify an unstable model of the system by a closed-loop step test. In this paper, we use the identified model for an IMC (Internal Model Control) design. Three IMC controllers are used to cover the operation range of the nonlinear system; for small, medium and large valve openings. Switching (gain-scheduling) between the three controllers is based on the pressure set-point.

This paper is organized as follows. A first principle model for sever-slugging is introduced in Section II. In Section III we present the state feedback and nonlinear observer. The model-based control with feedback linearization is introduced in Section IV. The model identification and IMC design are presented in Section V and the experiments are

978-1-4673-5716-6/13/$31.00 ©2013 IEEE

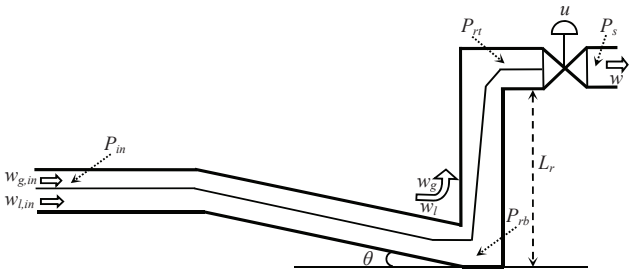

Fig. 1. Schematic presentation of system

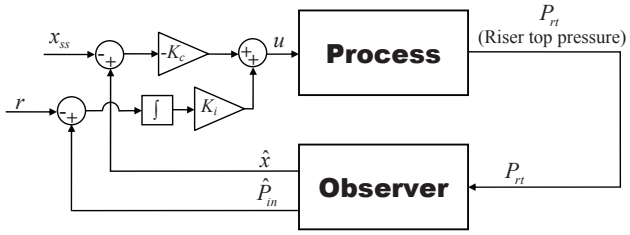

Fig. 2. Block diagram of closed-loop system

shown in Section VI. Finally, the main conclusions and remarks are summarized in Section VII.

II. FIRST PRINCIPLE MODEL

Fig. 1 shows a schematic presentation of the model. The inflow rates of gas and liquid to the system, $w_{g,in}$ and $w_{l,in}$, are assumed to be independent disturbances. The flow rates of gas and liquid from the pipeline to the riser, w_g and w_l, are determined by the pressure drop across the riser-base as described by virtual valve equations. The outlet mixture flow rate, w, is determined by the opening percentage of the top-side choke valve, $u = Z$, which is the manipulated variable of the control system.

For model-based control, we need a simplified model of the system. A PDE-based *two-fluid* model with 13 segments which results in a set of 50 ODEs was used in [9]. However, it was concluded that main dynamics can be captured by a simpler model. A four-state simplified model for severe-slugging flow in a pipeline-riser system was proposed in [10]. The state variables of this model are

- m_{gp}: mass of gas in pipeline [kg]
- m_{lp}: mass of liquid in pipeline [kg]
- m_{gr}: mass of gas in riser [kg]
- m_{lr}: mass of liquid in riser [kg]

The four main state equations of the model are

$$\dot{m}_{gp} = w_{g,in} - w_g \tag{1}$$

$$\dot{m}_{lp} = w_{l,in} - w_l \tag{2}$$

$$\dot{m}_{gr} = w_g - \alpha w \tag{3}$$

$$\dot{m}_{lr} = w_l - (1-\alpha) w \tag{4}$$

The flow rates and the gas mass fraction, α, in (1)-(4) are given by additional model equations provided in [10].

III. STATE FEEDBACK WITH NONLINEAR OBSERVER

As illustrated in Fig. 2, we want to estimate the state variables of the system by use of an observer. The *separation principle* which holds for linear systems allows us to separate the design into two tasks. First, we design a state feedback controller that stabilizes the system and meets other design specifications. Then an output feedback controller is obtained by replacing the state x by its estimate $\hat{x}$ provided by observers [11].

A. state-feedback

As shown in Fig. 2, we apply full state feedback by using estimated states. In addition, to prevent drift from the operating point, an integral action is added by using the estimated subsea pressure. The total control action can be expressed as

$$u(t) = -K_c(\hat{x}(t) - x_{ss}) + K_i \int_0^t (\hat{P}_{in}(\tau) - r) d\tau. \tag{5}$$

K_c is a linear optimal controller calculated by solving *Riccati equation* and K_i is a small integral gain (e.g. $K_i = 10^{-3}$).

B. Observer Design

A high-gain observer, under certain conditions, guarantees that the output feedback controller recovers the performance of the state feedback controller. The observer gain is designed so that the observer is robust to uncertainties in modeling the nonlinear functions. The structure of the simple high-gain observer is similar to the one used in [5]:

$$\begin{aligned} \dot{\hat{z}}_1 &= f_1(\hat{z}) \\ \dot{\hat{z}}_2 &= f_2(\hat{z}) \\ \dot{\hat{z}}_3 &= f_3(\hat{z}) + \frac{1}{\epsilon}(y - \hat{y}) \\ \dot{\hat{z}}_4 &= f_4(\hat{z}) \end{aligned} \tag{6}$$

where

- z_1, mass of gas in pipeline (m_{gp})
- z_2, mass of liquid in pipeline (m_{lp})
- z_3, pressure at top of riser (P_{rt})
- z_4, mass of liquid in riser (m_{lr})

and $\frac{1}{\epsilon}$ is the high gain. Three of equations (f_1, f_2 and f_4) are the same as the model in equations (1), (2) and (4). For the third state equation (f_3), we transform the state into the top pressure which is a measurement ($y = z_3$ and $\hat{y} = \hat{z}_3$). We select $z_3 = P_{rt}$, because it is directly related to the original third state of the model (m_{gr}, mass of gas in the riser):

$$P_{rt} = \frac{m_{gr} R T_r}{M_G \left(V_r - \frac{m_{lg}}{\rho_l} \right)} \tag{7}$$

We obtain the time derivative of the top pressure by using partial derivatives:

$$f_3(z) = \frac{dP_{rt}}{dt} \tag{8}$$

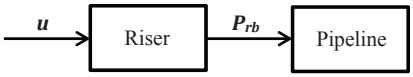

Fig. 3. Pipeline-riser system as a cascade connection of two subsystems

$$\frac{dP_{rt}}{dt} = \frac{\partial P_{rt}}{\partial m_{gr}}\dot{m}_{gr} + \frac{\partial P_{rt}}{\partial m_{lr}}\dot{m}_{lr} \tag{9}$$

where

$$\frac{\partial P_{rt}}{\partial m_{gr}} = \frac{a}{b - m_{lr}} \tag{10}$$

$$\frac{\partial P_{rt}}{\partial m_{lr}} = \frac{a m_{gr}}{(b - m_{lr})^2} \tag{11}$$

In (10) and (11), $a = RT_r\rho_l/M_G$ and $b = \rho_l V_r$ are model constants. See [10] for details of the model.

IV. OUTPUT LINEARIZING CONTROLLER

A nonlinear model-based controller using feedback linearization has been proposed in [7]. This controller directly uses the pressure at the riser-base (P_{rb}) and the pressure at the top of the riser (P_{rt}) as measurements, without any observer. We present a summary of the assumptions used for the controller design and the control law here. Details of the derivation and a proof for the closed-loop stability is provided in [7].

A. Cascade System Structure

In order to simplify the system analysis, we separate it into two subsystems. Then, we analyze the individual subsystems and their interconnecting relationships. As illustrated in Fig. 3, the input to the "Riser" subsystem (Σ_2) is the choke valve opening, $u = Z$, and the output is the pressure at the riser-base, P_{rb}, which is also the input to the "Pipeline" subsystem (Σ_1). Considering the riser-slugging instability, we state the following hypothesis about the "Pipeline" subsystem:

Hypothesis 1. The "Pipeline" subsystem with the riser-base pressure, P_{rb}, as its input is"input-to-state stable".

We investigate the input-to-state stability of the pipeline subsystem by a simulation test as shown in Fig. 4. The riser-base pressure in this simulation is 19.7 kPa. This pressure corresponds to 50% opening of the top-side valve ($Z = 50\%$) for which the non-slugging flow regime is unstable. However, the pipeline subsystem separated from the riser is always stable. The local exponential stability of the "Pipeline" subsystem can be verified by looking at its eigenvalues. The above hypothesis is reasonably correct, because the riser-base pressure is a recommended candidate controlled variable to stabilize the system [12]. This means when the riser-base pressure has small variations, the whole system becomes stabilized which follows $\mathcal{L}_2$-gain stability from P_{rb} to state variables of the pipeline subsystem.

We can now state the following proposition:

Proposition 1. Let hypothesis 1 hold. If the Riser subsystem becomes globally asymptotically stable under a stabilizing feedback control, then the pipeline-riser system is globally asymptotically stable.

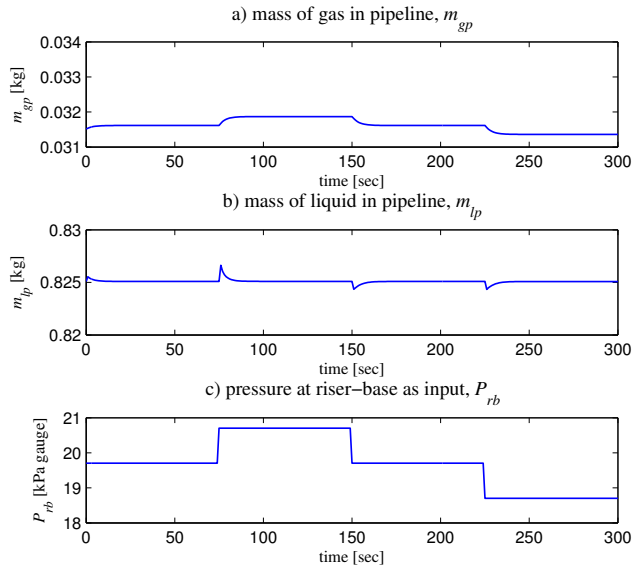

Fig. 4. Simulation test of pipeline subsystem

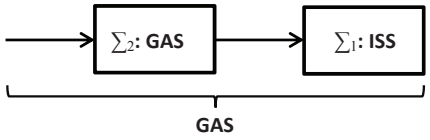

Fig. 5. Stability of a cascade system

Proof: We use conditions for stability of cascaded systems as stated by *Corollary 10.5.3* in [13]. As illustrated in Fig. 5, if Σ_1 is input-to-state stable (ISS) and the origin of Σ_2 is globally asymptotically stable (GAS), then the origin of the cascaded system Σ_1 and Σ_2 is globally asymptotically stable (GAS). Therefore, if *Hypothesis 1* holds, the proposition is verified.

It is not possible to achieve GAS for the riser subsystem due to controllability limitations and other physical limits of the system. Instead, we show partial stabilization with respect to the output that enters the pipeline subsystem, P_{rb}, on a set $\mathcal{D}$ which is the physical domain of the system [7].

B. Stabilizing Controller for Riser Subsystem

The two measurements used by the controller are $y_1 = P_{rb}$ and $y_2 = P_{rt}$.

$$F(y) = c\left(1 - \frac{y_2}{a}\right)\frac{a\alpha + y_2(1-\alpha)}{bc - (y_1 - y_2 - F_r)}, \tag{12}$$

where $c = gL_r/V_r$ and F_r is friction function for the riser which depends on the constant inflow rates and other constant parameters. We use the gas and liquid inflow rates to the system to calculate the gas mass fraction, α. Although it is different from the original model in (1)-(4), it is the same at steady-state:

$$\alpha = \frac{w_{g,in}}{w_{g,in} + w_{l,in}}. \tag{13}$$

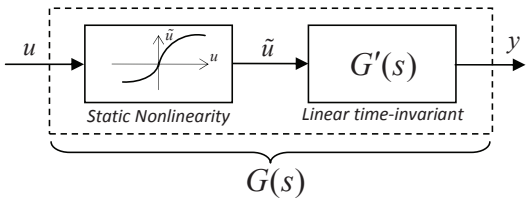

Fig. 6. Block diagram for Hammerstein model

The virtual control input is

$$w = \frac{w_{in}(F(y)+c) + K_1(y_1 - \bar{y}_1)}{F(y)+c}, \tag{14}$$

where $K_1 > 0$ and $w_{in} = w_{g,in} + w_{l,in}$ is the constant inlet flow rate to the system. $\bar{y}_1$ is the steady-state value or the set-point. The final control signal to the valve is

$$u = \text{sat}\left(\frac{w}{K_{pc}\sqrt{\rho_{rt}(y_2 - P_s)}}\right), \tag{15}$$

where K_{pc} and P_s are the choke valve constant and the separator pressure, respectively. The riser friction function F_r and the density ρ_{rt} are calculated based on the two pressure measurements y_1 and y_2 and model parameters (see [7]).

V. IMC DESIGN BASED ON IDENTIFIED MODEL

A. Model Identification

We use a Hammerstein model structure (Fig. 6) to describe the desired unstable operating point (flow regime). The Hammerstein model consists of a series connection of a static nonlinearity (gain K) and a linear time-invariant dynamic system, $G'(s)$. For identification of the unstable dynamics, we need to assume a structure. We first considered a simple unstable first-order plus delay model:

$$G(s) = \frac{Ke^{-\theta s}}{\tau s - 1} = \frac{be^{-\theta s}}{s - a} \tag{16}$$

where $a > 0$. If we control this system with a proportional controller with gain K_{c0} (Fig. 7), the closed-loop transfer function from the set-point (y_s) to the output (y) becomes

$$\frac{y(s)}{y_s(s)} = \frac{K_{c0}G(s)}{1 + K_{c0}G(s)} = \frac{K_{c0}be^{-\theta s}}{s - a + K_{c0}be^{-\theta s}}. \tag{17}$$

In order to get a stable closed-loop system, we need $K_{c0}b > a$. The steady-state gain of the closed-loop transfer function is then

$$\frac{\Delta y_\infty}{\Delta y_s} = \frac{K_{c0}b}{K_{c0}b - a} > 1. \tag{18}$$

However, the closed-loop experimental step response (see Fig. 8) shows that the steady-state gain is smaller than one. Therefore, the model form in (16) is not a correct choice.

If we linearize the four-state mechanistic model in (1)-(4) around the desired unstable operating point, we get a fourth-order linear model in the form

$$G(s) = \frac{\theta_1(s+\theta_2)(s+\theta_3)}{(s^2 - \theta_4 s + \theta_5)(s^2 + \theta_6 s + \theta_7)}. \tag{19}$$

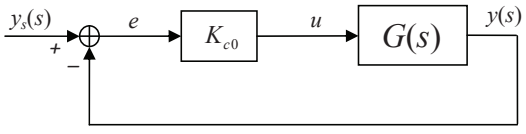

Fig. 7. Closed-loop system for step test

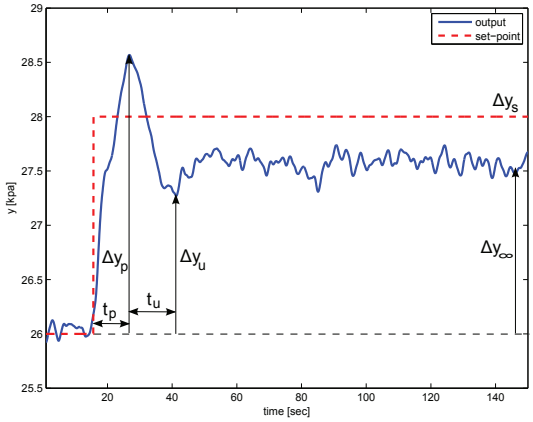

Fig. 8. Experimental closed-loop step response for system stabilized with proportional control

This model contains two unstable poles, two stable poles and two zeros. Seven parameters (θ_i) must be estimated to identify this model. However, if we look at the Hankel Singular Values of the fourth-order model (Fig. 9), we find that the stable part of the system has little dynamic contribution. This suggests that a model with two unstable poles is sufficient for control design. Using a model truncation (square root method), we obtained a reduced-order model in the form of

$$G(s) = \frac{b_1 s + b_0}{s^2 - a_1 s + a_0}, \tag{20}$$

where $a_0 > 0$ and $a_1 > 0$. The model has two unstable poles and four parameters, b_1, b_0, a_1 and a_0, need to be estimated. If we control the unstable process in (20) using a proportional controller with gain K_{c0}, the closed-loop transfer function from set-point (y_s) to output (y) becomes

$$\frac{y(s)}{y_s(s)} = \frac{K_{c0}(b_1 s + b_0)}{s^2 + (-a_1 + K_{c0}b_1)s + (a_0 + K_{c0}b_0)}. \tag{21}$$

This can be rewritten to the model used in [14]:

$$\frac{y(s)}{y_s(s)} = \frac{K_2(1+\tau_z s)}{\tau^2 s^2 + 2\zeta\tau s + 1} \tag{22}$$

To estimate the four parameters (K_2, τ_z, τ and ζ) in (22), we use six data (Δy_p, Δy_u, Δy_∞, Δy_s, t_p and t_u) observed from the closed-loop response (see Fig. 8). Then, we back-calculate the parameters of the open-loop unstable model in (20). Details are given in [15].

B. IMC design for unstable systems

The Internal Model Control (IMC) design procedure is summarized in [16]. The block diagram of the IMC structure

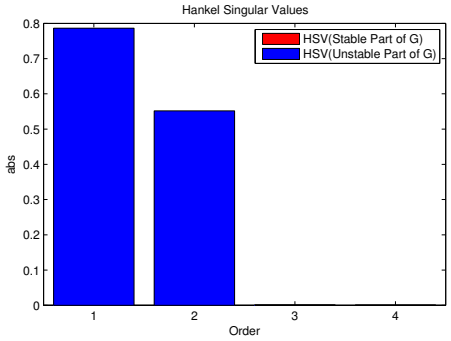

Fig. 9. Hankel Singular Values of fourth order model

is shown in Fig. 10. Here, $G(s)$ is the plant model which in general has some mismatch with the real plant $G_p(s)$. $\tilde{Q}(s)$ is the inverse of the minimum phase part of $G(s)$ and $f(s)$ is a low-pass filter for robustness of the closed-loop system. The IMC configuration in Fig. 10 cannot be used directly for unstable systems; instead we use the conventional feedback structure with the stabilizing controller

$$C(s) = \frac{\tilde{Q}(s)f(s)}{1 - G(s)\tilde{Q}(s)f(s)}. \tag{23}$$

For internal stability, $\tilde{Q}f$ and $(1 - G\tilde{Q}f)$ have to be stable. We use the identified model from the previous section as the plant model:

$$G(s) = \frac{\hat{b}_1 s + \hat{b}_0}{s^2 - \hat{a}_1 s + \hat{a}_0} = \frac{k'(s+\varphi)}{(s-\pi_1)(s-\pi_2)} \tag{24}$$

and we get

$$\tilde{Q}(s) = \frac{(1/k')(s-\pi_1)(s-\pi_2)}{s+\varphi} \tag{25}$$

We design the filter $f(s)$ as explained in [16]:
k = number of RHP poles + 1 = 3
m = max(number of zeros of $\tilde{Q}(s)$ *- number of pole of* $\tilde{Q}(s)$ *,1) = 1 (to make* $Q = \tilde{Q}f$ *proper)*
n = m + k -1 = 3 (filter order)

The filter is in the following from:

$$f(s) = \frac{\alpha_2 s^2 + \alpha_1 s + \alpha_0}{(\lambda s + 1)^3}, \tag{26}$$

where λ is an adjustable closed-loop time-constant. We choose $\alpha_0 = 1$ to get integral action and the coefficients α_1 and α_2 are calculated by solving the following system of linear equations:

$$\begin{pmatrix} {\pi_1}^2 & \pi_1 & 1 \\ {\pi_2}^2 & \pi_2 & 1 \end{pmatrix} \begin{pmatrix} \alpha_2 \\ \alpha_1 \\ \alpha_0 \end{pmatrix} = \begin{pmatrix} (\lambda\pi_1 + 1)^3 \\ (\lambda\pi_2 + 1)^3 \end{pmatrix} \tag{27}$$

Finally, from (23) the feedback version of the IMC controller becomes

$$C(s) = \frac{[\frac{1}{k'\lambda^3}](\alpha_2 s^2 + \alpha_1 s + 1)}{s(s+\varphi)}. \tag{28}$$

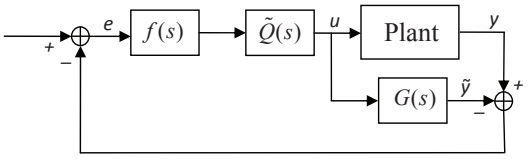

Fig. 10. Block diagram of Internal Model Control system

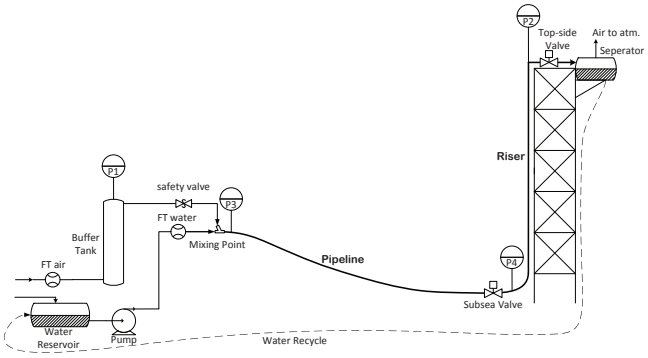

Fig. 11. Schematic diagram of experimental setup

VI. EXPERIMENTS

A. Experimental Setup

The experiments were performed in a laboratory setup for anti-slug control at the Chemical Engineering Department of NTNU. Fig. 11 shows a schematic presentation of the laboratory setup. The pipeline and the riser are made from flexible pipe with 2 cm inner diameter. The length of the pipeline is 4 m, and it is inclined with a 15° angle. The height of the riser is 3 m. A buffer tank is used to simulate the effect of a long pipe with the same volume, such that the total resulting length of inlet pipe would be about 70 m.

The topside choke valve is used as the input for control, $u = Z$. The separator pressure after the topside choke valve is at atmospheric pressure. The feed into the pipeline is assumed to be at constant flow rates; 4 $litre/min$ of water and 4.5 $litre/min$ of air. With these boundary conditions, the critical valve opening where the system switches from stable (non-slug) to oscillatory (slug) flow is at $Z^* = 15\%$. The bifurcation diagrams [9], shown in Fig. 12, are used to fit the nonlinear model (solid lines) to the experimental data (dashed lines).

The desired steady-state (middle line) is unstable for $Z > 15\%$, but it can be stabilized by using control. The slope of this steady-state line (in the middle) is the static gain of the system, $k = \partial y/\partial u = \partial P_{in}/\partial Z$. As the valve opening increase this slope decreases, and the gain approaches zero as $Z \to 100\%$. This makes control of the system with large valve openings very difficult.

B. Experimental results

All the experiments are performed with a set of descending pressure set-points to observe where the system becomes unstable. We repeated each experiments for three different

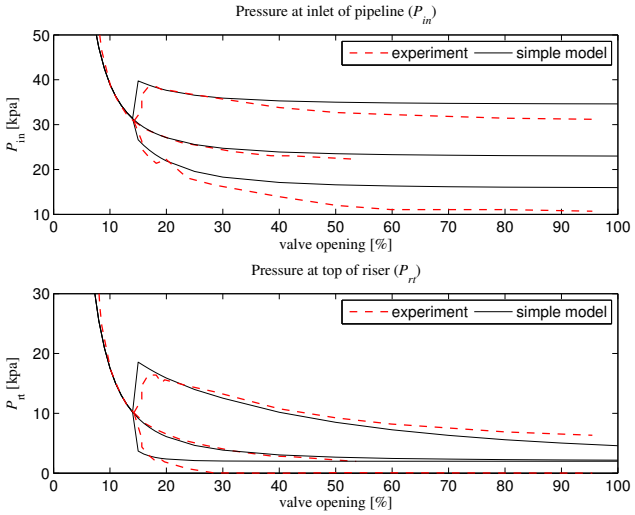

Fig. 12. Bifurcation diagrams of simplified model (solid) compared to experiments (dashed)

values of added time delay 1 *sec*, 2 *sec* and 3 *sec*, but we do not show results for 1 *sec* time-day because of space limitation. The time delay was added to the measured output.

Fig. 13 shows result of using the state feedback with nonlinear observer scheme for control. It can stabilize the system up to 28% valve opening. However, with 2 *sec* time delay, as in Fig. 14, it is stable only up to 22% valve opening. This scheme can stabilize the system only when using the top-side pressure P_{rt} as the measurement for the observer, since a high-gain observer diverges when using the subsea pressure P_{in} as the measurement (see Fig. 15). The reason for this has been explained in [6].

Fig. 16 shows result of using the feedback linearization controller. With no time delay, it stabilizes the system up to 60% valve opening. However, with 2 *sec* time delay, as in Fig. 17, it is stable only up to 25% valve opening.

Next, we identify three linear models from closed-loop step tests at three different operating points, $Z = 20\%$, $Z = 30\%$ and $Z = 40\%$, respectively,

$$G_1(s) = \frac{-0.015(\mathrm{s}+0.26)}{s^2 - 0.045s + 0.0094}, \tag{29}$$

$$G_2(s) = \frac{-0.0098(\mathrm{s}+0.25)}{s^2 - 0.040s + 0.025}, \tag{30}$$

$$G_3(s) = \frac{-0.0056(\mathrm{s}+0.27)}{s^2 - 0.017s + 0.096}. \tag{31}$$

Then, we design three IMC controllers for the three valve openings.

$$C_1(s) = \frac{-16.15(s^2 + 0.016s + 0.0012)}{\mathrm{s}(\mathrm{s}+0.26)} \tag{32}$$

$$C_2(s) = \frac{-42.20(s^2 + 0.052s + 0.0047)}{\mathrm{s}(\mathrm{s}+0.25)} \tag{33}$$

$$C_3(s) = \frac{-115.11(s^2 + 0.052s + 0.014)}{\mathrm{s}(\mathrm{s}+0.27)} \tag{34}$$

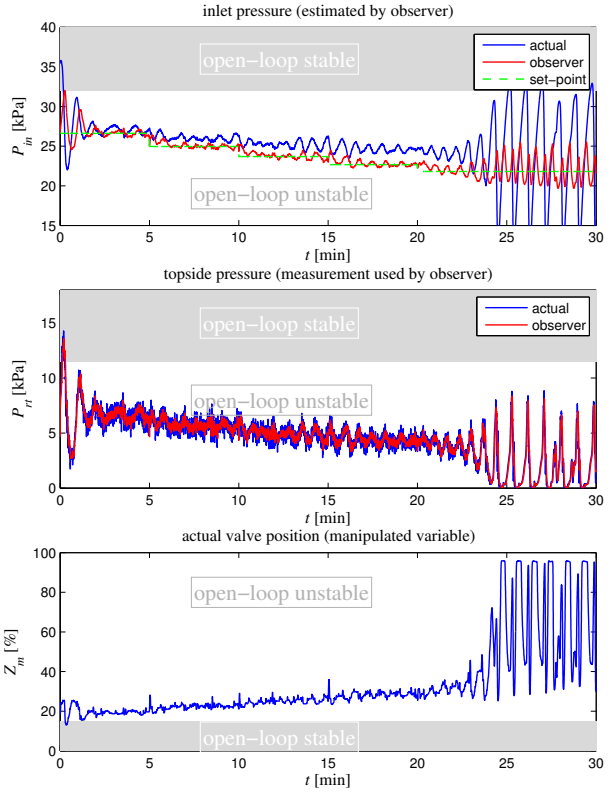

Fig. 13. Control using High-Gain observer with top pressure (P_{rt}) measured and no time delay

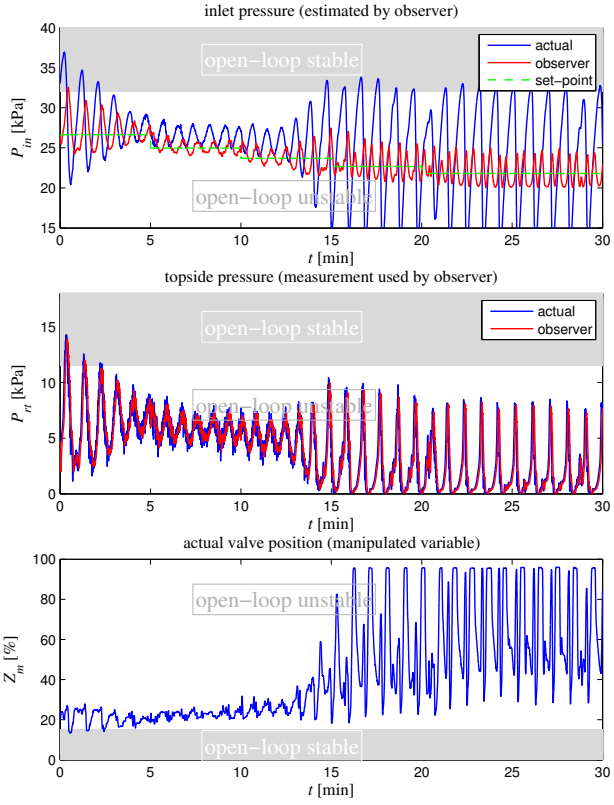

Fig. 14. Control using High-Gain observer with top pressure (P_{rt}) measured and 2 *sec* time delay

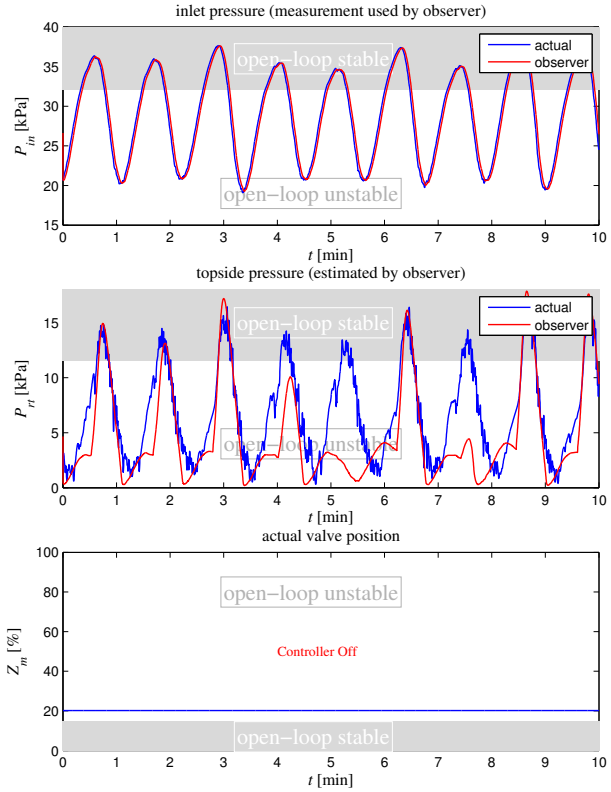

Fig. 15. Open-loop estimation using High-Gain observer with subsea pressure (P_{in}) measurement

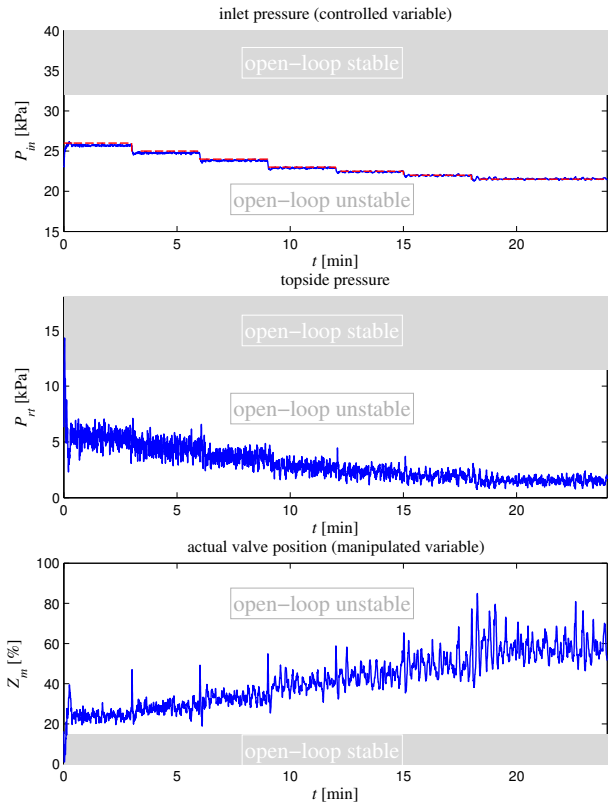

Fig. 16. Control using nonlinear controller with subsea pressure (P_{in}) measured and no time delay

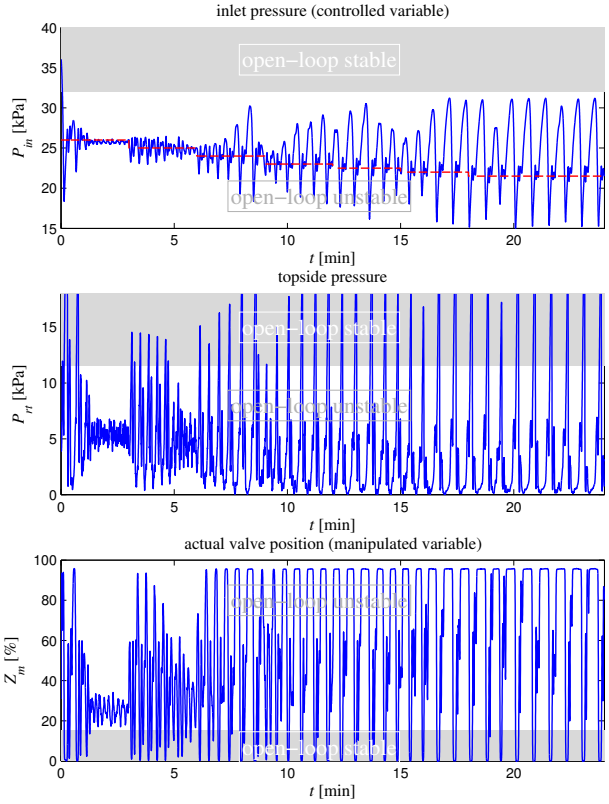

Fig. 17. Control using nonlinear controller with subsea pressure (P_{in}) measured and 2 *sec* time delay

TABLE II

GAIN-SCHEDULING LOGIC

Pressure set-point	Controller
$P_{set} \geq 24\ kPa$	$C_1(s)$
$24\ kPa > P_{set} > 21.5\ kPa$	$C_2(s)$
$P_{set} \leq 21.5\ kPa$	$C_3(s)$

Switching (gain-scheduling) between the three controllers is based on the pressure set-point as given in Table II, and bump-less transfer between controllers is included.

Fig. 18 shows result of applying gain scheduling IMC. This scheme stabilizes the system up to 60% valve opening, and even with 2 *sec* time delay (Fig. 19), it is stable up to 50% valve opening.

Table III shows the maximum valve opening achieved by using the three methods with different values of time-delay.

TABLE III

MAXIMUM VALVE OPENING ACHIEVED BY USING DIFFERENT CONTROLLERS AND DIFFERENT VALUES OF TIME DELAY

	$\theta = 0$	$\theta = 1$	$\theta = 2$
Gain-scheduling IMC	60%	60%	50%
Feedback linearization	60%	40%	25%
Nonlinear observer	28%	24%	22%

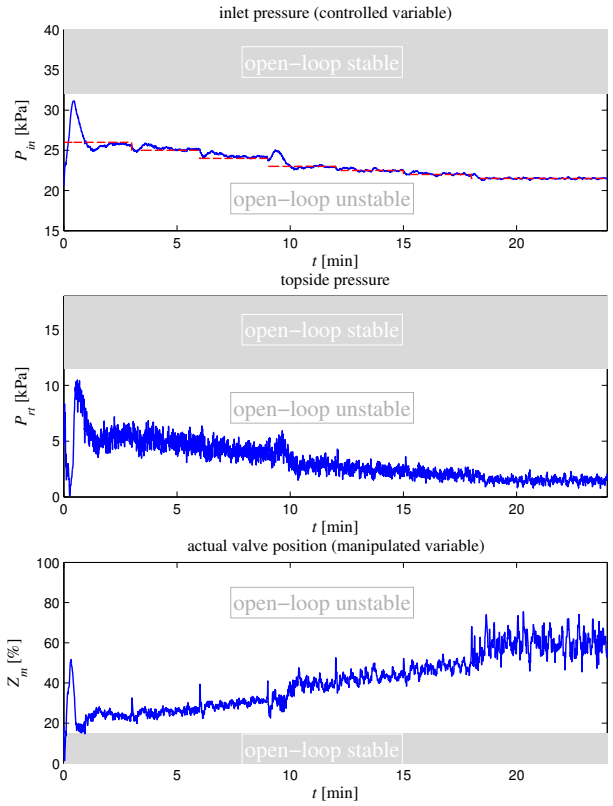

Fig. 18. Control using IMC controller with subsea pressure (P_{in}) measured and no time delay

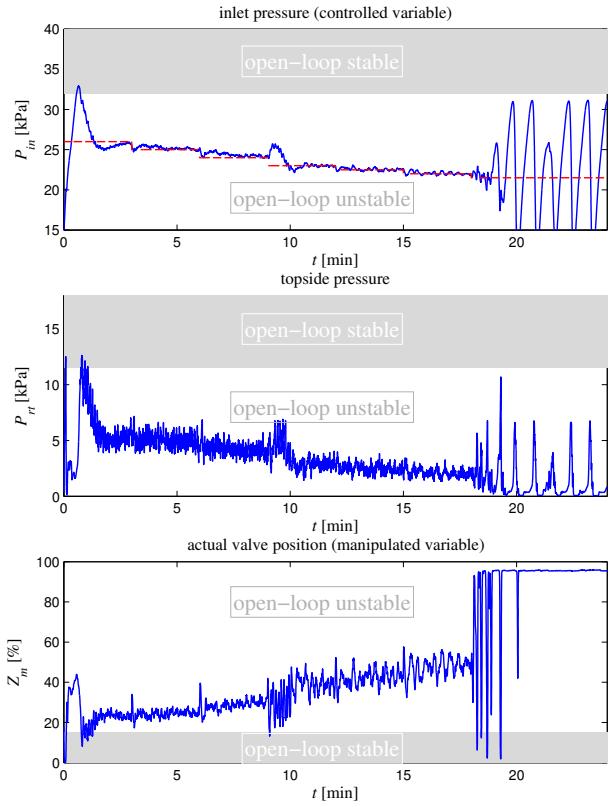

Fig. 19. Control using IMC controller with subsea pressure (P_{in}) measured and 2 *sec* time delay

VII. CONCLUSIONS

Two model-based controllers from the previous works of the authors, the state-feedback/nonlinear observer [6], the feedback linearizing controller [7], and a new gain-scheduling with IMC controllers based on model identification were tested in experiments. The gain-scheduling IMC was able to stabilize the system up to large valve openings even when adding time delay to control loop (time delay in the measurement is a major problem of long flow-lines). The IMC controller takes advantage of derivative action which results in a better phase-margin for stabilizing control, while the nonlinear model-based controllers are essentially proportional controllers. Other advantages of the IMC scheme are its simplicity and the fact that it is not directly designed based on the mechanistic model. It is based on identified models from closed-loop step responses. The second best controller for this case study is the feedback-linearizing controller which uses the measurements directly. The state-feedback/nonlinear observer scheme was able to stabilize the system in a very limited range.

REFERENCES

[1] K. Havre, K. Stornes, and H. Stray, "Taming slug flow in pipelines," *ABB Review*, vol. 4, pp. 55–63, 2000.

[2] H. Sivertsen, V. Alstad, and S. Skogestad, "Medium-scale experiments on stabilizing riser-slug flow," *SPE Projects, Facilities & Construction*, vol. 4, no. 4, pp. 156–170, SPE no. 120 040, 2009.

[3] G.-O. Kaasa, V. Alstad, J. Zhou, and O. M. Aamo, "Nonlinear model-based control of unstable wells," *Journal of Modeling, Identification and Control*, vol. 28, no. 3, pp. 69–79, 2007.

[4] F. Di Meglio, G.-O. Kaasa, N. Petit, and V. Alstad, "Model-based control of slugging flow: an experimental case study," in *American Control Conference*, Baltimore, USA, 2010, pp. 2995–3002.

[5] ——, "Reproducing slugging oscillations of a real oil well," in *49th IEEE Conference on Decision and Control*, Atlanta, Georgia, USA, 2010, pp. 4473–4479.

[6] E. Jahanshahi, S. Skogestad, and E. I. Grøtli, "Anti-slug control experiments using nonlinear observer," in *American Control Conference*, Washington D.C., 2013.

[7] ——, "Nonlinear model-based control of two-phase flow in risers by feedback linearization," in *9th IFAC Symposium on Nonlinear Control Systems*, Toulouse, France, 2013.

[8] E. Storkaas, "Stabilizing control and controllability: Control solutions to avoid slug flow in pipeline-riser system," Ph.D. dissertation, Norwegian University of Science and Technology, NTNU, 2005.

[9] E. Storkaas and S. Skogestad, "Controllability analysis of two-phase pipeline-riser systems at riser slugging conditions," *Control Engineering Practice*, vol. 15, no. 5, pp. 567–581, 2007.

[10] E. Jahanshahi and S. Skogestad, "Simplified dynamical models for control of severe slugging in multiphase risers," in *18th IFAC World Congress*, Milan, Italy, Auguest 2011, pp. 1634–1639.

[11] H. K. Khalil, *Nonlinear Systems, Third Edition*. Upper Saddle River, New Jersey: Prentice Hall, 2002.

[12] E. Jahanshahi, S. Skogestad, and A. H. Helgesen, "Controllability analysis of severe slugging in well-pipeline-riser systems," in *IFAC Workshop - Automatic Control in Offshore Oil and Gas Production*, Trondheim, Norway, May 2012, pp. 101–108.

[13] A. Isidori, *Nonlinear Control Systems II*, 1st ed. London: Springer-Verlag, 1999.

[14] M. Yuwana and D. E. Seborg, "A new method for on-line controller tuning," *AIChE Journal*, vol. 28, no. 3, pp. 434–440, May 1982.

[15] E. Jahanshahi and S. Skogestad, "Closed-loop model identification and pid/pi tuning for robust anti-slug control," in *10th IFAC International Symposium on Dynamics and Control of Process Systems*, Mumbai, India, 2013.

[16] M. Morari and E. Zafiriou, *Robust Process Control*. Englewood Cliffs, New Jersey: Prentice Hall, 1989.